

DOSE: Data Selection for Multi-Modal LLMs via Off-the-Shelf Models

Anonymous ACL submission

Abstract

Large-scale multimodal data have greatly accelerated the progress of vision-language models. However, selecting high-quality and diverse training data under limited data budgets remains an under-explored problem. We propose DOSE, a novel data selection pipeline that uses off-the-shelf models—without any fine-tuning on the target corpus—to independently evaluate text quality and image–text alignment. These scores are combined into a joint quality–alignment distribution, from which we apply adaptive weighted random sampling to select informative samples while preserving long-tail diversity. Extensive experiments on general VQA and math benchmarks show that DOSE enables a flexible trade-off between model performance and data selection efficiency. Remarkably, DOSE achieves near full-dataset performance using only 20% of the original data, and can even surpass the full-dataset baseline when using larger subsets. Since DOSE only requires inference-time computation and no additional fine-tuning, it is particularly suitable for resource-constrained settings and fast model development cycles.

1 Introduction

Visual instruction tuning has been widely adopted for training MLLMs (Liu et al., 2023; Bai et al., 2023), enabling these models to understand language instructions based on visual content. Current approaches typically rely on collecting or synthesizing large instruction tuning datasets to improve the model capabilities (Zhao et al., 2023; Wang et al., 2024a; Shi et al., 2024; Nguyen et al., 2023). These datasets, while effective, lead to increased computational resource strain and high costs in model development due to its enormous volume. Inspired by (Zhou et al., 2023), which showed that a high-quality subset of data can deliver performance comparable to that of full-scale data, we aim to develop

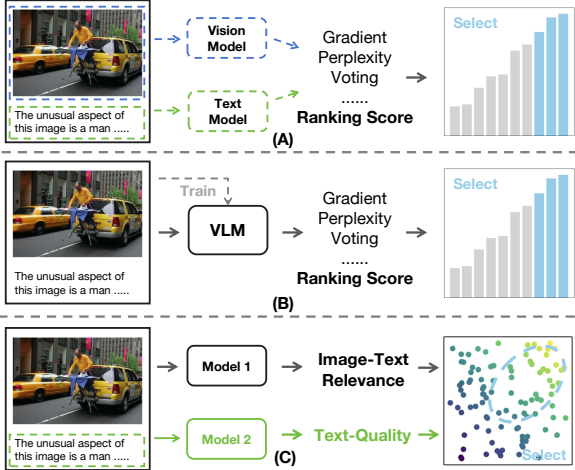


Figure 1: **Comparison of data selection methods.** (A) The methods that rely on a single metric from either vision or text model (dashed line). (B) The methods that leverage VLMs for data quality assessment. Notably, the VLMs are already trained on the target data that will be filtered. (C) Our approach constructs data distribution by harnessing existing pre-trained models that have not been exposed to the target data.

a data selection method that retains only the most valuable examples. This method should substantially reduce computational cost, while maintaining or even exceeding the performance of models trained on the full dataset.

Effective multimodal data selection consists of two interdependent components—quality assessment and sampling strategy. Quality assessment encompasses (1) lightweight, model-agnostic cues such as early-training loss norms in EL2N (Paul et al., 2021) and confidence margins in Self-Filter (Chen et al., 2024), and (2) sophisticated, model-driven measures such as gradient-influence scores in LESS (Cao et al., 2023), multi-task consensus in ICONS (Wu et al., 2024b), and small-model activation grouping in COINCIDE (Lee et al., 2024). Lightweight metrics add negligible overhead but suffer from ignoring high-value long-

tail examples (Marion et al., 2023a), which degrades downstream accuracy; by contrast, gradient-based and clustering approaches yield more precise quality estimates yet demand costly backward passes or expensive clustering pipelines that undermine overall efficiency. Sampling strategies add another layer of complexity: fixed-threshold filters hoard only the highest-scoring samples (Cao et al., 2023), neglecting mid-range and tail instances (Wu et al., 2024a); stratified or weighted schemes rely on fragile density or distribution estimates that magnify biases when miscalculated; and iterative, multi-round pipelines only compound inefficiencies (Wu et al., 2024b). Critically, most techniques validate exclusively on near-domain splits and offer scant insight into true cross-domain or long-tail generalization (Lee et al., 2024), leaving the development of efficient, semantically diverse, and robust selection strategies for novel domains still largely unexplored.

To balance downstream accuracy, computational cost, and cross-domain generalization, we introduce a two-stage pipeline. In the first stage—the Quality Scoring via Off-the-Shelf Models—we leverage instruction-tuned LLMs with carefully engineered prompts to assign each long text or question–answer pair an approval probability (Sachdeva et al., 2024), and use a vision–language matching network to compute an alignment score for every image–caption pair (Hessel et al., 2021). Both metrics require only a single forward pass, avoiding any backward propagation or additional training, and leverage their rich pre-trained representations to produce quality estimates with strong cross-domain generalization. In the second stage—Weighted Random Sampling—we fit empirical density estimates to these approval and alignment scores, then perform adaptive weighted sampling: higher-scoring samples are proportionally more likely to be selected, while every score interval—including low-density long-tail regions—retains a nonzero chance of inclusion. This two-stage approach produces a compact, information-rich coreset that preserves rare but valuable examples, matches or exceeds full-dataset performance on both near-domain and truly unseen tasks, and enables rapid, resource-efficient training without sacrificing robustness or semantic diversity.

We conducted extensive evaluations on general VQA benchmarks and specialized math tasks, using LLaVA-1.5-7B and LLaVA-1.5-13B as base-

lines. Remarkably, with only 20 % of the data, DOSE retains 96 % of full-data performance on general VQA with 20 % of the data and even surpasses full-data results on math tasks using 20 % subset. Moreover, in terms of both efficiency and performance, DOSE outperforms methods that require prior exposure to the filtered data, demonstrating a superior balance of performance, computational cost, cross-domain generalization, and sample diversity.

Our contributions are summarized as follows:

- We propose DOSE, a data selection method for multimodal LLMs. It leverages existing pre-trained, off-the-shelf models to evaluate text quality and image-text relevance, thereby identifying high-quality training samples.
- Extensive experiments demonstrate that our method consistently outperforms various baselines. By leveraging Pareto optimality, our method achieves advanced performance in both effectiveness and efficiency.
- Further experiments on multimodal math benchmarks validate that our approach can generalize well to the training data in specialized domain and merely a small fraction of training data can achieve comparable performance of full training set.

2 Related Work

2.1 Data Quality Scoring

Quality-score was originally developed for importance sampling but is now widely used in training LLMs. The scoring algorithm evaluates sample importance using various methods, including measuring disagreement rates between models (Chitta et al., 2021), assessing whether a sample is likely to be "forgotten" (Toneva et al., 2019), "memorized" (Feldman and Zhang, 2020), or "unlearnable" (Mindermann et al., 2022), and applying perplexity filtering to prioritize low-perplexity samples while discarding high-perplexity ones (Wenzek et al., 2019; Marion et al., 2023b; Muenighoff et al., 2023). Recent advancements have enabled perplexity estimation through efficient model-based simulators, eliminating the need for full LLM inference (Guu et al., 2023). Additionally, some approaches select training data by minimizing the distance between the selected data distribution and

high-quality sources such as Wikipedia or books. This is often achieved through contrastive classifiers or feature-space matching (Radford et al., 2019; Anil et al., 2023; Javaheripi et al., 2023). To more effectively assess the comprehensive quality of multimodal image-text data, we introduce the CLIP-Score (Hessel et al., 2021) for evaluating image-text relevance. For textual data, we leverage the reasoning capabilities of instruction-tuned LLMs to directly evaluate sample quality. Specifically, we use the acceptance probability assigned by the LLM to measure the likelihood that a given text is valid and meaningful.

2.2 Data Selection on Distribution

Data selection is crucial for improving model training quality and can be divided into two categories: distribution-agnostic filtering and distribution-aware selection. Distribution-agnostic methods focus on the quality of individual samples, typically using thresholds to identify subsets. For example, these methods may detect mismatched text-image pairs or misleading elements in images. Specifically, (Nguyen et al., 2023; Mahmoud et al., 2023) employ BLIP to identify mismatches between captions and images, while (Maini et al., 2023) leverage OCR models to filter images where text is the only feature correlated with the caption. In contrast, distribution-aware methods optimize subset selection by statistically analyzing the overall data distribution. Classical techniques, such as those proposed in (Wei et al., 2015; Raskutti and Mahoney, 2016; Coleman et al., 2019), aim to maximize subset performance under a fixed budget. More recently, (Wang et al., 2023) introduced an approach that replaces traditional models with a trained codebook, clusters samples, and selects representative samples from each cluster. Our method builds upon these ideas by constructing a joint distribution of image-text relevance and text quality. We carefully analyze the impact of different regions and diversity within this joint distribution on data quality, ultimately selecting the most representative samples for training.

3 Methodology

Multimodal data selection mainly focuses on assessment data quality, with existing methods typically assessing text quality and the overall quality of image-text pairs. To achieve comprehensive quality assessment, we combine these methods and

create a unified scoring strategy. Existing text quality evaluation methods either introduce bias toward noisy samples with information or face the issue where the evaluation model has already seen the data during training. To address this, we introduce the Text-Quality Score, which leverages the reasoning capabilities of a pre-trained LLM to assess text quality. Additionally, we use the widely adopted CLIP-Score to evaluate the quality of image-text pairs. Meanwhile, selecting data using a static threshold may lead to a loss of diversity and the discarding of valuable edge cases, potentially limiting performance. To address this, we introduce a weighted sampling strategy that integrates data diversity with score-based selection. This approach enables us to select a high-quality subset while maintaining stability and representativeness, ensuring both performance and diversity are preserved.

3.1 Off-the-Shelf Quality Assessment

We leverage the reasoning capabilities of pre-trained LLMs and multimodal language models to evaluate data quality. Inspired by Ask-LLM (Sachdeva et al., 2024), we prompt the LLM to predict whether an input sample is suitable for fine-tuning a multimodal language model. As illustrated in Table 3, the LLM predicts “yes” when the text is informative, well-formatted, and aligned with visual instruction tuning objectives. The softmax probability assigned to the “yes” token serves as the *Text-Quality Score* for the sample.

In addition, similar to (Nguyen et al., 2023; Mahmoud et al., 2023; Maini et al., 2023; Fang et al., 2023), we use the CLIP-ViT-B32 (OpenAI, 2023) to obtain CLIP-Score (Hessel et al., 2021) to assess the alignment between images and their captions. The CLIP model projects both images and text into a shared embedding space, and the cosine similarity between these embeddings quantitatively measures the image-text relevance.

3.2 Weighted Random Sampling

After obtaining the Text-Quality (x_i) and Image-Text Relevance Scores (y_i), we can use Kernel Density Estimation (*KDE*) to establish the density distribution of the data. We define this distribution as the original distribution $p(x)$. And, to better accommodate high-quality data in terms of x_i and y_i , we construct a new distribution for Weighted Random Sampling (*WRS*). We refer to this new distribution as the target distribution $q(x)$, and by performing random sampling from $q(x)$, we obtain

the final sampling results.

Sampling Procedure First, we compute the statistical properties of the original data, including the mean μ_{data} and standard deviation σ_{data} . Next, we use *KDE* to fit the probability density function of the original data:

$$KDE(x) = \frac{1}{Nh} \sum_{i=1}^N K\left(\frac{x - x_i}{h}\right), \quad (1)$$

where $K(\cdot)$ is the Gaussian kernel, N is the number of samples, and h is the bandwidth. We first remove outliers via DBSCAN (label = -1), then compute the KDE on the remaining data and locate its principal mode:

$$\mu_{\text{peak_kde}} = \arg \max_{x \in [x_{\min}, x_{\max}]} KDE(x). \quad (2)$$

Next, let

$$\mu_{\text{DB}} = \max_{i: \ell_i \neq -1} x_i,$$

where ℓ_i is the DBSCAN label for x_i . We then set the final target center to

$$\mu_{\text{peak_wrs}} = \frac{\mu_{\text{peak_kde}} + \mu_{\text{DB}}}{2}.$$

Based on $\mu_{\text{peak_wrs}}$, we model the target distribution $q(x)$ and the original distribution $p(x)$ as Gaussians with means $\mu_{\text{peak_wrs}}$ and μ_p , respectively.

Based on this, we define the target distribution $q(x)$ and the original distribution $p(x)$ as normal distributions with the following probability density functions:

$$\begin{aligned} q(x) &= \mathcal{N}(x; \mu_{\text{peak_wrs}}, \sigma_{\text{data}}), \\ p(x) &= \mathcal{N}(x; \mu_p, \sigma_{\text{data}}). \end{aligned} \quad (3)$$

where μ_{peak} is the mean of the target distribution, and σ_{data} is the standard deviation (consistent with the original data). To perform WRS, we calculate the weight for each data point x_i as the ratio of the probability density under the target distribution to that under the original distribution:

$$w_i = \frac{q(x_i)}{p(x_i) + \epsilon}, \quad (4)$$

where $\epsilon = 10^{-10}$ is a small constant added to avoid division by zero. Subsequently, we normalize the weights:

$$w'_i = \frac{w_i}{\sum_{j=1}^N w_j}. \quad (5)$$

Finally, based on the normalized weights w'_i , we perform weighted random sampling to select M samples (without replacement) from the original data:

$$S_x = \{x_{i_1}, x_{i_2}, \dots, x_{i_M}\}, \quad (6)$$

where i_k are indices randomly drawn according to the weights w'_i . Through these steps, we generate a new sample set S that better aligns with the characteristics of the target distribution $q(x)$. Also, based on the Image-Text Relevance Scores (y_i), we can apply the same sampling strategy to obtain the corresponding subset:

$$S_y = \{y_{i_1}, y_{i_2}, \dots, y_{i_M}\}, \quad (7)$$

Combined Sampling Once the positions of all data points are determined in a two-dimensional coordinate space—where each point is defined by x_i (text quality) and y_i (image-text relevance)—we construct a density-like distribution that captures the frequency of data points within local regions. This distribution reveals patterns in the data, enabling us to analyze and compare the data distribution before and after sampling. Based on this distribution, we design a sampling strategy that prioritizes regions with both high densities and favorable characteristics in terms of x_i and y_i . Specifically, we define subsets S_x and S_y , which capture key features along the x_i and y_i dimensions, respectively. By combining the intersection of S_x and S_y , we derive the final sampling results.

$$DOSE = \{(x_i, y_i) \mid (x_i, y_i) \in S_x \cap S_y\}. \quad (8)$$

This approach ensures that the sampled points not only reflect the underlying data distribution but also align with preferred ranges for text quality and image-text relevance.

4 Experiments

In this section, we first describe our implementation and benchmark setups, then present results on VLM evaluations and ablation studies. We assess general VQA performance across nine benchmarks (see the Appendix for dataset details) and, following ICONS and COINCIDE, report the average relative performance (Rel.) to quantify cross-benchmark generalization.

Method	VQAv2	GQA	VizWiz	SQA-I	TextVQA	POPE	MME	MMBench en	MMBench cn	LLaVA-W Bench	Rel. (%)
Full	79.1	63.0	47.8	68.4	58.2	86.4	1476.9	66.1	58.9	67.9	100
<i>Methods that already used full data before data selection</i>											
COINCIDE	76.5	59.8	46.8	69.2	55.6	86.1	1495.6	63.1	54.5	67.3	97.4
ICONS	76.3	60.7	50.1	70.8	55.6	87.5	1485.7	63.1	55.8	66.1	98.6
<i>Methods that never used full data before data selection</i>											
Random	75.7	57.6	44.7	66.5	54.2	84.1	1389.0	62.2	54.8	65.0	94.5
CLIP-Score	73.4	51.4	43.0	65.0	54.7	85.3	1331.6	55.2	52.0	66.2	91.2
EL2N	76.2	58.7	43.7	65.5	53.0	84.3	1439.5	53.2	47.4	64.9	92.0
Perplexity	75.8	57.0	47.8	65.1	52.8	82.6	1341.4	52.0	45.8	<u>68.3</u>	91.6
SemDeDup	74.2	54.5	46.9	65.8	<u>55.5</u>	84.7	1376.9	52.2	48.5	70.0	92.6
D2-Pruning	73.0	58.4	41.9	<u>69.3</u>	51.8	85.7	1391.2	65.7	57.6	63.9	94.8
Self-Sup	74.9	59.5	46.0	<u>67.8</u>	49.3	83.5	1335.9	61.4	53.8	63.3	93.4
Self-Filter	73.7	58.3	53.2	61.4	52.9	83.8	1306.2	48.8	45.3	64.9	90.9
Ours	77.3	58.6	46.5	67.2	54.4	83.6	1462.2	62.5	54.8	65.8	96.0

Table 1: **Comparisons with baseline methods.** For a fair comparison, all models are trained by 20% of full training data and the data subsets are selected by different methods. The best and second best results for each benchmark are shown in **bold** and underlined, respectively. Our method achieves the highest relative performance (98.6%), consistently outperforming existing methods, including COINCIDE (97.4%) (Lee et al., 2024) and D2-Pruning (94.8%) (Maharana et al., 2023), while methods like EL2N (Paul et al., 2021), Perplexity (Marion et al., 2023a), and CLIP-Score (Hessel et al., 2021) show limited effectiveness with relative performance around 91-92%.

4.1 Setup

Implementation Details Our method has been validated on both pre-training and downstream tasks for VLMs. For the pre-training task, we follow the settings of LLaVA-1.5-7b (Liu et al., 2023) and score and filter the data in stage 2 of LLaVA, retrain stage 2, and compare the performance differences across various data scales and filtering methods. For the downstream task, we follow the settings of Math-LLaVA (Wang et al., 2024b) and apply the same method to score and filter the MathV360k (Shi et al., 2024) dataset. Based on the pre-trained LLaVA-1.5-13b (Liu et al., 2023), we perform continuous fine-tuning. In the Text-Quality Scoring phase, we score the 665k text data using Vicuna-7b (Team, 2023), obtaining its original distribution. Based on this distribution, we adaptively fit a WRS sampling. Similarly, we use CLIP-Score (Hessel et al., 2021) to obtain another distribution and perform sampling. By combining this with the proposed combined sampling strategy, we obtain the final sampling results, which are used for the main results.

4.2 Main Results

Comparisons with Baselines We compare our DOSE against a suite of established data-selection methods using a 20 % subset of LLaVA-1.5’s Stage-2 data, shown in Table 2. Baselines in-

clude Random sampling; CLIP-Score (Hessel et al., 2021) for image-text alignment; EL2N (Paul et al., 2021) based on embedding L2 norms; Perplexity (Marion et al., 2023a) from language-model likelihoods; SemDeDup (Abbas et al., 2023) for semantic deduplication; D2-Pruning (Maharana et al., 2023) for distribution-aware pruning; and Self-Sup (Sorscher et al., 2022) leveraging self-supervised signals. We also include vision-language-specific approaches Self-Filter (Chen et al., 2024) and COINCIDE (Lee et al., 2024). DOSE achieves the highest overall relative performance (96.0 %), surpassing all unseen-selection baselines by over 1 pp—e.g., improving on D2-Pruning (94.8 %)—and closing the gap to seen-data methods like ICONS (98.6 %) to just 2.6 pp. Notably, DOSE outperforms Random on every benchmark (e.g., GQA: 58.6 vs 57.6; TextVQA: 54.4 vs 54.2) and matches or exceeds stronger baselines across tasks from VQA-v2 through MMBench, demonstrating its ability to select a small, high-value subset that nearly rivals full-data finetuning.

While DOSE achieves strong unseen-data selection performance (96.0 % Rel.), it trails seen-data methods such as ICONS (Wu et al., 2024b) (98.6 %) and COINCIDE (Lee et al., 2024) (97.4 %). The reason is that those approaches first fine-tune on the full dataset and then use their own learned model parameters to rank or cluster samples, giving

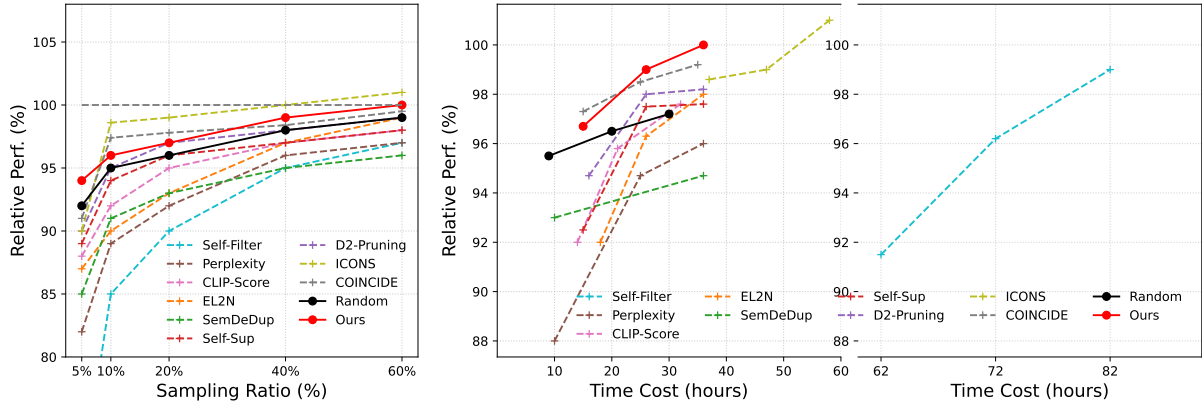


Figure 2: DOSE Data-Selection Efficiency and Wall-Clock Time Trade-Offs. (Left) Average relative performances of all coreset selection techniques at different sampling ratios for the LLaVA-1.5 dataset. (Right) Comparison of coreset selection techniques on average relative performance and wall-clock time cost. The wall-clock time cost includes both the data selection and finetuning of the target LVLm. The time cost is measured in hours of running time on a computing node with 4×V100 GPUs.

395 them direct access to downstream performance sig- 426
 396 nals. In contrast, DOSE relies only on off-the-shelf 427
 397 pre-trained models—no additional finetuning—so 428
 398 it cannot leverage those proprietary performance 429
 399 cues. However, this independence from any prelim- 430
 400 inary full-data training is also DOSE’s key advan- 431
 401 tage: it avoids the redundant, expensive pass over 432
 402 the entire dataset purely for selection purposes, dra- 433
 403 matically reducing computation and resource costs 434
 404 while still delivering near-state-of-the-art results 435
 405 on much smaller subsets. 436

406 **Different Selection Ratio.** As shown in Figure 437
 407 4, we compare DOSE (red solid line with circles) 438
 408 against ten baselines—Random (black), Perplex- 439
 409 ity (Marion et al., 2023a), CLIP-Score (Hessel 440
 410 et al., 2021), EL2N (Paul et al., 2021), SemD- 441
 411 eDup (Abbas et al., 2023), Self-Sup (Sorscher et al., 442
 412 2022), D2-Pruning (Maharana et al., 2023), COIN- 443
 413 CIDE (Lee et al., 2024), ICONS (Wu et al., 2024b), 444
 414 and Self-Filter—across sampling ratios from 5 % to 445
 415 60 %. DOSE rapidly climbs to 99 % Rel. by 40 % 446
 416 sampling, matching or exceeding all other unseen- 447
 417 data methods and even approaching the seen-data 448
 418 ICONS (Wu et al., 2024b) curve at higher ratios. 449

419 **Pareto Superior.** Among all data selection base- 450
 420 lines shown in Figure 4, DOSE achieves the 451
 421 largest performance gains among methods that do 452
 422 not rely on prior exposure to the training data, 453
 423 outperforming baselines such as Random, CLIP- 454
 424 Score, EL2N, SemDeDup, Perplexity, Self-Sup, 455
 425 D2-Pruning, and Self-Filter by 1–4 percentage 456
 457

426 points under identical sampling ratios and time 427
 428 budgets. Even against the two leading seen-data 429
 430 methods, ICONS and COINCIDE, DOSE holds 431
 432 clear advantages. ICONS and COINCIDE both 433
 434 require an expensive full-data fine-tuning pass be- 435
 436 fore sample selection—a cost that would recur for 436
 437 any new dataset yet is omitted from their reported 437
 438 compute comparisons—whereas DOSE skips this 438
 439 phase entirely, relying solely on off-the-shelf pre- 439
 440 trained models for scoring and weighted sampling. 440
 441 As a result, direct comparisons of compute costs are 441
 442 misleading. Moreover, DOSE’s linear-time scoring 442
 443 lets it reach 97.4 % relative performance in 12 h 443
 444 and 98.5 % in 22 h, whereas COINCIDE needs 15 444
 445 h/97.4 % and 25 h/98.4 %, and ICONS—lacking 445
 446 a time-optimized pipeline—lags further behind. Fi- 446
 447 nally, DOSE requires no clustering hyperparam- 447
 448 eters, gradient-influence computations, or extra 448
 449 network training—its runtime scales linearly with 449
 450 dataset size and is immediately deployable—while 450
 451 seen-data methods add complexity that complicates 451
 452 tuning and extension. 452

448 **Unseen-task Generalization.** As shown in Table 448
 449 2, we filtered the MathV360K (Shi et al., 2024) 449
 450 dataset and performed continuous fine-tuning on 450
 451 LLaVA-1.5-13B (Liu et al., 2023) using high- 451
 452 quality subsets of varying proportions. In this pro- 452
 453 cess, we strictly adhered to the experimental set- 453
 454 tings of Math-LLaVA (Shi et al., 2024). Since the 454
 455 evaluation on MathVista requires GPT-3.5 (Brown 455
 456 et al., 2020) to extract key results, and the perfor- 456
 457 mance of different period versions may vary, we 457

Size	Math-LLaVA on MathVista													
	FQA	GPS	MWP	TQA	VQA	ALG	ARI	GEO	LOG	NUM	SCI	STA	Rel.%	Aver.
<i>Random selection on MathV360K</i>														
5%	22.7	38.0	30.7	41.1	38.6	36.7	31.4	38.1	21.6	30.6	38.5	23.9	88.4	32.7
20%	30.9	44.2	42.9	39.9	33.5	39.9	36.5	43.9	28.8	27.8	45.1	29.6	98.7	36.9
40%	32.3	52.4	43.0	37.3	35.2	45.6	35.7	52.3	16.2	27.8	41.9	35.9	97.6	38.0
<i>DOSE selection on MathV360K</i>														
5%	33.4	38.9	30.1	36.1	34.1	36.3	29.5	36.8	24.3	26.4	36.1	31.9	88.4	32.8
10%	30.5	39.9	33.9	39.9	31.8	37.4	30.0	40.2	16.2	26.7	40.2	31.9	86.8	33.2
20%	33.1	45.7	45.7	42.4	36.9	43.1	38.5	45.2	29.7	31.3	41.0	35.9	104.8	39.1
40%	32.7	49.5	47.3	43.7	34.6	47.0	37.1	49.4	18.9	27.8	40.2	37.5	100.4	38.8
65%	30.5	49.5	53.8	42.4	29.1	44.8	37.4	48.5	8.1	24.3	41.9	37.5	93.1	37.3
80%	32.4	53.4	49.5	45.6	36.3	48.4	39.4	51.9	16.2	27.8	46.7	38.2	103.5	40.5
100% [†]	37.9	52.8	46.8	44.3	27.9	48.4	33.2	51.9	18.9	23.6	45.1	41.9	100	39.4

Table 2: **Comparison with different data selection scales on domain-specific benchmarks.** [†] represents our reproduced results of Math-LLaVA-13B. The best results in all tasks are in bold. MathVista is divided in two ways: task type or mathematical skill, and we report the accuracy under each subset. Rel.% keep same setting with general benchmarks, and Aver. means the average score of all tasks.

reproduced the results of Math-LLaVA as a benchmark for comparison. The experimental results demonstrate that our method achieves performance comparable to Math-LLaVA (Shi et al., 2024) when using only 20% of the high-quality data. Furthermore, when using 80% of the data, the overall performance of the model improves by 1 percentage point. This demonstrates that the knowledge embedded in CLIP (Hessel et al., 2021) and Vicuna7B (Team, 2023), which we used for data filtering, is sufficiently comprehensive to not only select high-quality general data but also be effectively applied in special domains.

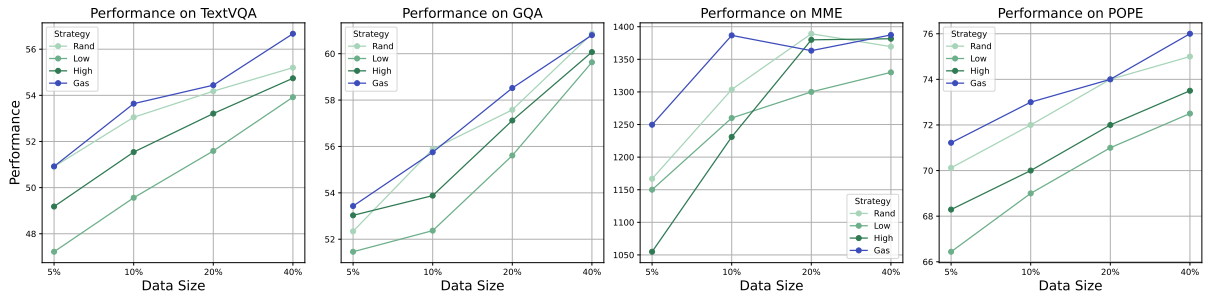
4.3 Ablation Study

In this section, we conduct ablation experiments by comparing different scoring strategies, score-based sampling strategies, and the fusion of these two strategies. The results are presented in Figure 3a, Figure 3b, and Figure 4 in Appendix.

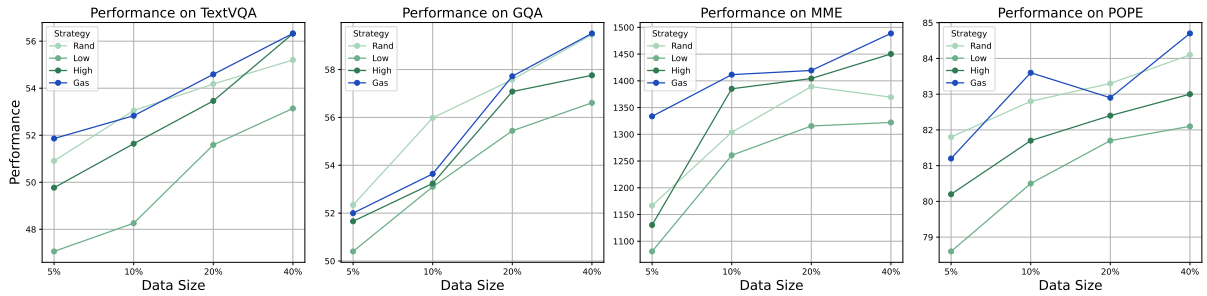
Effectiveness of Single Methods To verify the effectiveness of Text-Quality and CLIP scores individually, we first validated the data selection results of each method in Stage 2 of the LLaVA training program, as shown in Figure 3a. We compared four strategies based on the Text-Quality Score: the “Rand” strategy, which randomly samples from the entire dataset; the “High” strategy, which samples data above a certain threshold based on a scoring method; the “Low” strategy, which samples data

below a threshold; and the “Gas” strategy, which combines the overall data distribution with the high-score threshold and uses an adaptive Gaussian function for WRS sampling. When evaluating and sampling text data, performance generally improved as the data size increased from 5% to 40%, but the effectiveness of the strategies varied. Overall, the “High” strategy consistently outperformed the “Low” strategy, demonstrating that Text-Quality Score can effectively assess data quality. However, with smaller data sizes, the “High” strategy performed worse than “Rand” indicating that diversity is more important than quality when the data size is small. By combining WRS sampling and balancing both diversity and quality, the “Gas” strategy outperformed “Rand,” confirming the effectiveness of the data selection method.

In our evaluation of image-text relevance, shown in Figure 3b, we compared four sampling strategies using the CLIP Score. The results revealed that the “Gas” strategy significantly outperformed the others. This suggests that as the filtering ratio decreases, data quality differences become more noticeable, making it suitable for large datasets with low usage needs. However, as the dataset size grows, the differences in quality between filtered and unfiltered data become smaller. We also found that in the GQA task, the data filtered by CLIP Score did not show significant advantages, likely because the original data already had strong image-text relevance. This highlights a limitation of CLIP



(a) Performance comparison of different strategies based on Text-Quality Score on TextVQA, GQA, MME, and POPE datasets.



(b) Performance comparison of different strategies based on CLIP-Score on TextVQA, GQA, MME, and POPE datasets.

Figure 3: Overall performance comparisons across different strategies and datasets. (a) and (b) correspond to ablation studies on individual selection strategy based on Text-Quality Score and CLIP-Score.

Score in selecting certain datasets. To address this issue, we recommend using a combined sampling approach for a better assessment of data quality.

Effectiveness of Combined Sampling As shown in Figure 4, we identified 9 candidate regions based on the original data distribution. These regions represent clusters of data, reflecting the similarities and differences among samples. To create the combined distribution sampling data, we randomly sampled 5% of the overall data from each candidate region. This method ensures diversity in the samples while effectively capturing the underlying structure of the data. After constructing the combined distribution sampling data, we trained the model using the same settings as the single-method approach and tested it on several datasets, including TextQA (Singh et al., 2019a), GQA (Hudson and Manning, 2019a), POPE (Li et al., 2023a), and MME (Fu et al., 2023). And, the performance results are shown in Figure 4, which indicate that in the upper right area—where both CLIP and Text-Quality Score are high—the model generally performs better. This suggests that in general task, the combination of the two sampling methods can effectively select data that helps improve the model’s performance. By using this combined sampling method based on the distribution, we enhance the

representativeness and quality of the data, thereby improving the model’s training efficiency.

5 Conclusion

In this work, we proposed DOSE, an efficient and practical method for selecting data for multimodal instruction tuning. DOSE uses off-the-shelf models to separately score text quality and image–text alignment, and combines them into a joint quality–alignment distribution. Using adaptive weighted random sampling, DOSE selects informative samples while preserving data diversity. Experimental results show that DOSE achieves a strong balance between model performance and data selection cost. On both general tasks and specialized math benchmarks, DOSE reaches the performance of full-dataset training using only 20% of the data, and even surpasses it when using 40% to 80% subsets. Compared to existing methods, DOSE outperforms unseen-data selection strategies in both effectiveness and efficiency. Importantly, DOSE operates entirely at inference time and does not require any fine-tuning, significantly reducing time and computational cost. These findings highlight the importance of high-quality data selection in multimodal learning and demonstrate that DOSE is a scalable and practical solution, especially for resource-constrained environments.

6 Limitations

While our method demonstrates strong performance and high efficiency, our study is constrained by the experimental cost and a limited exploration budget. We evaluated only an array of sampling ratios and primarily tested our method on LLaVA-1.5 models (7B & 13B), without assessing more fine-grained sampling ratios or more types of models. As a result, the generality of DOSE across additional sampling ratios and diverse architectures remains to be validated in future work.

References

Amro Abbas, Kushal Tirumala, Dániel Simig, Surya Ganguli, and Ari S Morcos. 2023. Semdedup: Data-efficient learning at web-scale through semantic deduplication. *arXiv preprint arXiv:2303.09540*.

Rie Kubota Ando and Tong Zhang. 2005. A framework for learning predictive structures from multiple tasks and unlabeled data. *Journal of Machine Learning Research*, 6:1817–1853.

Galen Andrew and Jianfeng Gao. 2007. Scalable training of L1-regularized log-linear models. In *Proceedings of the 24th International Conference on Machine Learning*, pages 33–40.

Rohan Anil, Andrew M. Dai, Orhan Firat, Melvin Johnson, Dmitry Lepikhin, Alexandre Passos, Siamak Shakeri, Emanuel Taropa, Paige Bailey, and Zhifeng Chen et al. 2023. *Palm 2 technical report*. *Preprint*, arXiv:2305.10403.

Jinze Bai, Shuai Bai, Shusheng Yang, Shijie Wang, Sinan Tan, Peng Wang, Junyang Lin, Chang Zhou, and Jingren Zhou. 2023. Qwen-vl: A frontier large vision-language model with versatile abilities. *CoRR*, abs/2308.12966.

Tom Brown, Benjamin Mann, Nick Ryder, Melanie Subbiah, Jared D Kaplan, Prafulla Dhariwal, Arvind Neelakantan, Pranav Shyam, Girish Sastry, Amanda Askell, and 1 others. 2020. Language models are few-shot learners. *Advances in neural information processing systems*, 33:1877–1901.

Liangliang Cao, Bowen Zhang, Chen Chen, Yinfei Yang, Xianzhi Du, Wencong Zhang, Zhiyun Lu, and Yantao Zheng. 2023. Less is more: Removing text-regions improves clip training efficiency and robustness. *arXiv preprint arXiv:2305.05095*.

Ruibo Chen, Yihan Wu, Lichang Chen, Guodong Liu, Qi He, Tianyi Xiong, Chenxi Liu, Junfeng Guo, and Heng Huang. 2024. Your vision-language model itself is a strong filter: Towards high-quality instruction tuning with data selection. *arXiv preprint arXiv:2402.12501*.

Kashyap Chitta, José M Álvarez, Elmar Haussmann, and Clément Farabet. 2021. Training data subset search with ensemble active learning. *IEEE Transactions on Intelligent Transportation Systems*, 23(9):14741–14752.

Cody Coleman, Christopher Yeh, Stephen Mussmann, Baharan Mirzasoleiman, Peter Bailis, Percy Liang, Jure Leskovec, and Matei Zaharia. 2019. Selection via proxy: Efficient data selection for deep learning. *arXiv preprint arXiv:1906.11829*.

Alex Fang, Albin Madappally Jose, Amit Jain, Ludwig Schmidt, Alexander Toshev, and Vaishaal Shankar. 2023. Data filtering networks. *arXiv preprint arXiv:2309.17425*.

Vitaly Feldman and Chiyuan Zhang. 2020. What neural networks memorize and why: Discovering the long tail via influence estimation. *Advances in Neural Information Processing Systems*, 33:2881–2891.

Chaoyou Fu, Peixian Chen, Yunhang Shen, Yulei Qin, Mengdan Zhang, Xu Lin, Zhenyu Qiu, Wei Lin, Jinrui Yang, Xiawu Zheng, Ke Li, Xing Sun, and Rongrong Ji. 2023. Mme: A comprehensive evaluation benchmark for multimodal large language models. *arXiv preprint arXiv:2306.13394*.

Chaoyou Fu, Peixian Chen, Yunhang Shen, Yulei Qin, Mengdan Zhang, Xu Lin, Jinrui Yang, Xiawu Zheng, Ke Li, Xing Sun, Yunsheng Wu, and Rongrong Ji. 2024. *Mme: A comprehensive evaluation benchmark for multimodal large language models*. *Preprint*, arXiv:2306.13394.

Yash Goyal, Tejas Khot, Douglas Summers-Stay, Dhruv Batra, and Devi Parikh. 2017. Making the v in vqa matter: Elevating the role of image understanding in visual question answering. In *Proceedings of the IEEE conference on computer vision and pattern recognition*, pages 6904–6913.

Danna Gurari, Qing Li, Abigale J Stangl, Anhong Guo, Chi Lin, Kristen Grauman, Jiebo Luo, and Jeffrey P Bigham. 2018. Vizwiz grand challenge: Answering visual questions from blind people. In *Proceedings of the IEEE conference on computer vision and pattern recognition*, pages 3608–3617.

Kelvin Guu, Albert Webson, Ellie Pavlick, Lucas Dixon, Ian Tenney, and Tolga Bolukbasi. 2023. Simfluence: Modeling the influence of individual training examples by simulating training runs. *arXiv preprint arXiv:2303.08114*.

Jack Hessel, Ari Holtzman, Maxwell Forbes, Ronan Le Bras, and Yejin Choi. 2021. Clipscore: A reference-free evaluation metric for image captioning. *arXiv preprint arXiv:2104.08718*.

Drew A Hudson and Christopher D Manning. 2019a. Gqa: A new dataset for real-world visual reasoning and compositional question answering. In *Proceedings of the IEEE/CVF conference on computer vision and pattern recognition*, pages 6700–6709.

679	Drew A Hudson and Christopher D Manning. 2019b.	Max Marion, Ahmet Üstün, Luiza Pozzobon, Alex	734
680	Gqa: A new dataset for real-world visual reasoning	Wang, Marzieh Fadaee, and Sara Hooker. 2023b.	735
681	and compositional question answering. In <i>Proceed-</i>	When less is more: Investigating data pruning	736
682	ings of the <i>IEEE/CVF conference on computer vision</i>	for pretraining llms at scale. <i>arXiv preprint</i>	737
683	and <i>pattern recognition</i> , pages 6700–6709.	<i>arXiv:2309.04564</i> .	738
684	Mojan Javaheripi, Sébastien Bubeck, Marah Abdin, Jy-	Sören Mindermann, Jan M Brauner, Muhammed T Raz-	739
685	oti Aneja, Sebastien Bubeck, Caio César Teodoro	zak, Mrinank Sharma, Andreas Kirsch, Winnie Xu,	740
686	Mendes, Weizhu Chen, Allie Del Giorno, Ronen El-	Benedikt Hölten, Aidan N Gomez, Adrien Morisot,	741
687	dan, Sivakanth Gopi, and 1 others. 2023. Phi-2: The	Sebastian Farquhar, and 1 others. 2022. Prioritized	742
688	surprising power of small language models.	training on points that are learnable, worth learning,	743
689	Jaewoo Lee, Boyang Li, and Sung Ju Hwang. 2024.	and not yet learnt. In <i>International Conference on</i>	744
690	Concept-skill transferability-based data selection	<i>Machine Learning</i> , pages 15630–15649. PMLR.	745
691	for large vision-language models. <i>arXiv preprint</i>	Niklas Muennighoff, Alexander M Rush, Boaz Barak,	746
692	<i>arXiv:2406.10995</i> .	Teven Le Scao, Aleksandra Piktus, Nouamane Tazi,	747
693	Yifan Li, Yifan Du, Kun Zhou, Jinpeng Wang,	Sampo Pyysalo, Thomas Wolf, and Colin Raffel.	748
694	Wayne Xin Zhao, and Ji-Rong Wen. 2023a. Eval-	2023. Scaling data-constrained language models.	749
695	uating object hallucination in large vision-language	<i>arXiv preprint arXiv:2305.16264</i> .	750
696	models. <i>arXiv preprint arXiv:2305.10355</i> .	Thao Nguyen, Samir Yitzhak Gadre, Gabriel Ilharco,	751
697	Yifan Li, Yifan Du, Kun Zhou, Jinpeng Wang,	Sewoong Oh, and Ludwig Schmidt. 2023. Improv-	752
698	Wayne Xin Zhao, and Ji-Rong Wen. 2023b. Eval-	ing multimodal datasets with image captioning. <i>Ad-</i>	753
699	uating object hallucination in large vision-language	<i>advances in Neural Information Processing Systems</i> ,	754
700	models. <i>Preprint</i> , arXiv:2305.10355.	36:22047–22069.	755
701	Haotian Liu, Chunyuan Li, Yuheng Li, and Yong Jae	OpenAI. 2023. Gpt-4 technical report . <i>Preprint</i> ,	756
702	Lee. 2023. Improved baselines with visual instruc-	arXiv:2303.08774.	757
703	tion tuning. <i>arXiv preprint arXiv:2310.03744</i> .	Mansheej Paul, Surya Ganguli, and Gintare Karolina	758
704	Pan Lu, Hritik Bansal, Tony Xia, Jiacheng Liu, Chun-	Dziugaite. 2021. Deep learning on a data diet: Find-	759
705	yuan Li, Hannaneh Hajishirzi, Hao Cheng, Kai-	ing important examples early in training. <i>Advances</i>	760
706	Wei Chang, Michel Galley, and Jianfeng Gao. 2023.	in <i>Neural Information Processing Systems</i> , 34:20596–	761
707	Mathvista: Evaluating math reasoning in visual con-	20607.	762
708	texts with gpt-4v, bard, and other large multimodal	Alec Radford, Jeffrey Wu, Rewon Child, David Luan,	763
709	models . <i>CoRR</i> , abs/2310.02255.	Dario Amodei, Ilya Sutskever, and 1 others. 2019.	764
710	Pan Lu, Swaroop Mishra, Tony Xia, Liang Qiu, Kai-	Language models are unsupervised multitask learn-	765
711	Wei Chang, Song-Chun Zhu, Oyvind Tafjord, Peter	ers. <i>OpenAI blog</i> , 1(8):9.	766
712	Clark, and Ashwin Kalyan. 2022. Learn to explain:	Garvesh Raskutti and Michael W Mahoney. 2016. A sta-	767
713	Multimodal reasoning via thought chains for science	tistical perspective on randomized sketching for ordi-	768
714	question answering. In <i>The 36th Conference on Neu-</i>	nary least-squares. <i>The Journal of Machine Learning</i>	769
715	<i>ral Information Processing Systems (NeurIPS)</i> .	<i>Research</i> , 17(1):7508–7538.	770
716	Adyasha Maharana, Prateek Yadav, and Mohit Bansal.	Mohammad Sadegh Rasooli and Joel R. Tetreault. 2015.	771
717	2023. D2 pruning: Message passing for balancing di-	Yara parser: A fast and accurate dependency parser .	772
718	versity and difficulty in data pruning. <i>arXiv preprint</i>	<i>Computing Research Repository</i> , arXiv:1503.06733.	773
719	<i>arXiv:2310.07931</i> .	Version 2.	774
720	Anas Mahmoud, Mostafa Elhoushi, Amro Abbas,	Noveen Sachdeva, Benjamin Coleman, Wang-Cheng	775
721	Yu Yang, Newsha Ardalani, Hugh Leather, and Ari	Kang, Jianmo Ni, Lichan Hong, Ed H Chi, James	776
722	Morcos. 2023. Sieve: Multimodal dataset prun-	Caverlee, Julian McAuley, and Derek Zhiyuan Cheng.	777
723	ing using image captioning models. <i>arXiv preprint</i>	2024. How to train data-efficient llms. <i>arXiv preprint</i>	778
724	<i>arXiv:2310.02110</i> .	<i>arXiv:2402.09668</i> .	779
725	Pratyush Maini, Sachin Goyal, Zachary C Lipton, J Zico	Wenhao Shi, Zhiqiang Hu, Yi Bin, Junhua Liu, Yang	780
726	Kolter, and Aditi Raghunathan. 2023. T-mars: Im-	Yang, See-Kiong Ng, Lidong Bing, and Roy Ka-Wei	781
727	proving visual representations by circumventing text	Lee. 2024. Math-LLaVA: Bootstrapping mathemat-	782
728	feature learning. <i>arXiv preprint arXiv:2307.03132</i> .	ical reasoning for multimodal large language models .	783
729	Max Marion, Ahmet Üstün, Luiza Pozzobon, Alex	In <i>Findings of the Association for Computational</i>	784
730	Wang, Marzieh Fadaee, and Sara Hooker. 2023a.	<i>Linguistics: EMNLP 2024</i> , pages 4663–4680, Mi-	785
731	When less is more: Investigating data pruning	ami, Florida, USA. Association for Computational	786
732	for pretraining llms at scale. <i>arXiv preprint</i>	Linguistics.	787
733	<i>arXiv:2309.04564</i> .		

788	Amanpreet Singh, Vivek Natarajan, Meet Shah,	Bo Zhao, Boya Wu, Muyang He, and Tiejun Huang.	842
789	Yu Jiang, Xinlei Chen, Dhruv Batra, Devi Parikh,	2023. Svit: Scaling up visual instruction tuning.	843
790	and Marcus Rohrbach. 2019a. Towards vqa models	<i>arXiv preprint arXiv:2307.04087</i> .	844
791	that can read. In <i>Proceedings of the IEEE/CVF con-</i>		
792	<i>ference on computer vision and pattern recognition</i> ,	Chunting Zhou, Pengfei Liu, Puxin Xu, Srinivasan Iyer,	845
793	pages 8317–8326.	Jiao Sun, Yuning Mao, Xuezhe Ma, Avia Efrat, Ping	846
		Yu, Lili Yu, and 1 others. 2023. Lima: Less is more	847
794	Amanpreet Singh, Vivek Natarajan, Meet Shah,	for alignment. <i>Advances in Neural Information Pro-</i>	848
795	Yu Jiang, Xinlei Chen, Dhruv Batra, Devi Parikh,	<i>cessing Systems</i> , 36:55006–55021.	849
796	and Marcus Rohrbach. 2019b. Towards vqa models		
797	that can read. In <i>Proceedings of the IEEE/CVF con-</i>	A Benchmarks	850
798	<i>ference on computer vision and pattern recognition</i> ,		
799	pages 8317–8326.	GQA (Hudson and Manning, 2019b), which fo-	851
		uses on reasoning about visual attributes like color	852
800	Ben Sorscher, Robert Geirhos, Shashank Shekhar, Surya	and shape, and VQA-v2 (Goyal et al., 2017), which	853
801	Ganguli, and Ari Morcos. 2022. Beyond neural scal-	assesses broader visual reasoning. MME (Fu et al.,	854
802	ing laws: beating power law scaling via data pruning.	2024) evaluates both perceptual abilities and cog-	855
803	<i>Advances in Neural Information Processing Systems</i> ,	nitive reasoning, while TextVQA (Singh et al.,	856
804	35:19523–19536.	2019b) tests OCR-based reasoning. POPE (Li et al.,	857
		2023b) addresses object hallucination, assessing	858
805	The Vicuna Team. 2023. Vicuna: An open-source	models’ ability to avoid generating non-existent	859
806	chatbot impressing gpt-4 with 90%* chatgpt quality.	objects. VizWiz (Gurari et al., 2018) focuses on	860
807	https://lmsys.org/blog/2023-03-30-vicuna .	basic visual reasoning for users who are blind, and	861
		ScienceQA (Lu et al., 2022) evaluates knowledge-	862
808	M. Toneva, A. Sordoni, R. Combes, A. Trischler, Y. Ben-	grounded question answering. Together, these	863
809	gio, and G. Gordon. 2019. An empirical study of ex-	benchmarks provide a comprehensive test of rea-	864
810	ample forgetting during deep neural network learning.	soning, perception, and understanding. Meanwhile,	865
811	In <i>ICLR</i> .	for the Special VQA task, we use MathVista (Lu	866
		et al., 2023), a benchmark designed to assess math-	867
812	Alex Jinpeng Wang, Kevin Qinghong Lin, David Junhao	ematical reasoning in visual contexts. It comprises	868
813	Zhang, Stan Weixian Lei, and Mike Zheng Shou.	6,141 questions from various datasets and covers	869
814	2023. Too large; data reduction for vision-language	categories such as FQA, GPS, MWP, TQA, and	870
815	pre-training. <i>arXiv preprint arXiv:2305.20087</i> .	VQA. With a focus on arithmetic, algebra, and	871
		logic, MathVista includes a diverse range of image	872
816	Bin Wang, Fan Wu, Xiao Han, Jiahui Peng, Huaping	types, making it an essential platform for evaluating	873
817	Zhong, Pan Zhang, Xiaoyi Dong, Weijia Li, Wei	models’ capabilities in mathematical reasoning.	874
818	Li, Jiaqi Wang, and 1 others. 2024a. Vige: Visual		
819	instruction generation and correction. In <i>Proceedings</i>	B Result Analysis	875
820	<i>of the AAAI Conference on Artificial Intelligence</i> ,		
821	volume 38, pages 5309–5317.	To understand how our proposed data selection	876
		strategy enhances training performance and effi-	877
822	Ke Wang, Junting Pan, Weikang Shi, Zimu Lu, Mingjie	ciency, we conducted a visualization and analysis	878
823	Zhan, and Hongsheng Li. 2024b. Measuring mul-	of the data used in LLaVA stage 2, consisting of	879
824	timodal mathematical reasoning with math-vision	665k data points. In the left panel of Figure 5, we	880
825	dataset. <i>arXiv preprint arXiv:2402.14804</i> .	plotted the CLIP-Score and Text-Quality Score for	881
		each data point, revealing a significant concentra-	882
826	Kai Wei, Rishabh Iyer, and Jeff Bilmes. 2015. Submod-	tion of data points in the central area. This suggests	883
827	ularity in data subset selection and active learning. In	that the data likely follows a normal distribution in	884
828	<i>International conference on machine learning</i> , pages	both scores, indicating regions of higher data qual-	885
829	1954–1963. PMLR.	ity. These insights led us to examine performance	886
		variations across different regions, as discussed in	887
830	Guillaume Wenzek, Marie-Anne Lachaux, Alexis Con-	Section 4.3. We found that areas with higher con-	888
831	neau, Vishrav Chaudhary, Francisco Guzmán, Ar-	centrations of data points generally correlated with	889
832	mand Joulin, and Edouard Grave. 2019. Ccnet: Ex-	better performance. This understanding drove us	890
833	tracting high quality monolingual datasets from web		
834	crawl data. <i>arXiv preprint arXiv:1911.00359</i> .		
835	Biao Wu, Fang Meng, and Ling Chen. 2024a. Cur-		
836	riculum learning with quality-driven data selection.		
837	<i>arXiv preprint arXiv:2407.00102</i> .		
838	Xindi Wu, Mengzhou Xia, Rulin Shao, Zhiwei Deng,		
839	Pang Wei Koh, and Olga Russakovsky. 2024b. Icons:		
840	Influence consensus for vision-language data selec-		
841	tion. <i>arXiv preprint arXiv:2501.00654</i> .		

891 to combine these insights with WRS to create a
892 high-quality data subset selection strategy.

893 We then visualized the distributions resulting
894 from random sampling (light blue) and WRS sam-
895 pling (light green) in the right panel of Figure
896 5. The WRS sampling distribution shows a pro-
897 nounced concentration in regions with higher CLIP
898 and Text-Quality Scores, effectively validating our
899 strategy for assessing data quality and demonstrat-
900 ing the benefits of our sampling approach.

Tasks	Examples of Task Templates
Original Template	Question: " <i><image></i> What are the colors of the bus in the image? " Answer: " The bus in the image is white and red. "
Scoring Template	Question: " ### What are the colors of the bus in the image? The bus in the image is white and red. ### Does the previous paragraph demarcated within ### contain informative signal for visual instruction tuning a vision-language model? An informative data point should be well-formatted, contain usable knowledge of the world, and strictly NOT have any harmful, racist, sexist, etc. content. OPTIONS: -yes -no " Answer: " Response: yes"

Table 3: Task template examples. "Original Template" represents the original format of the data, while "Scoring Template" represents the format used to assist in evaluating the quality of the text within the data. *<image>* indicates that the original data contains corresponding image information; in the scoring template, we only assess the quality of the textual information, so this token is omitted.

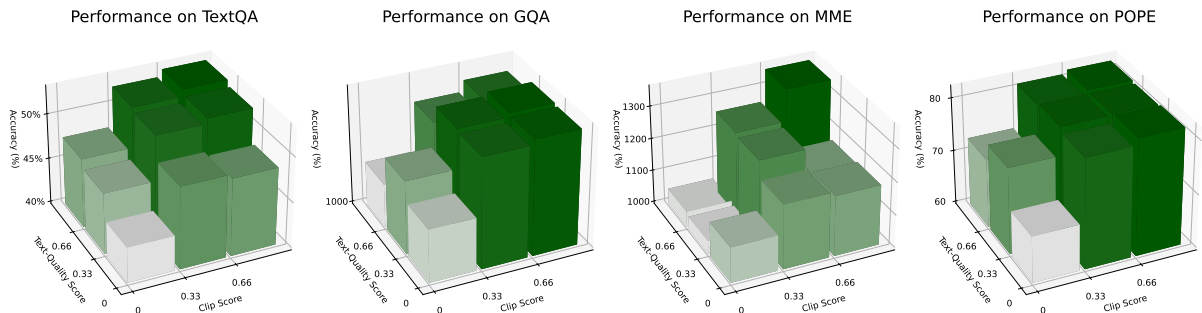


Figure 4: Performance comparison of different part datasets.

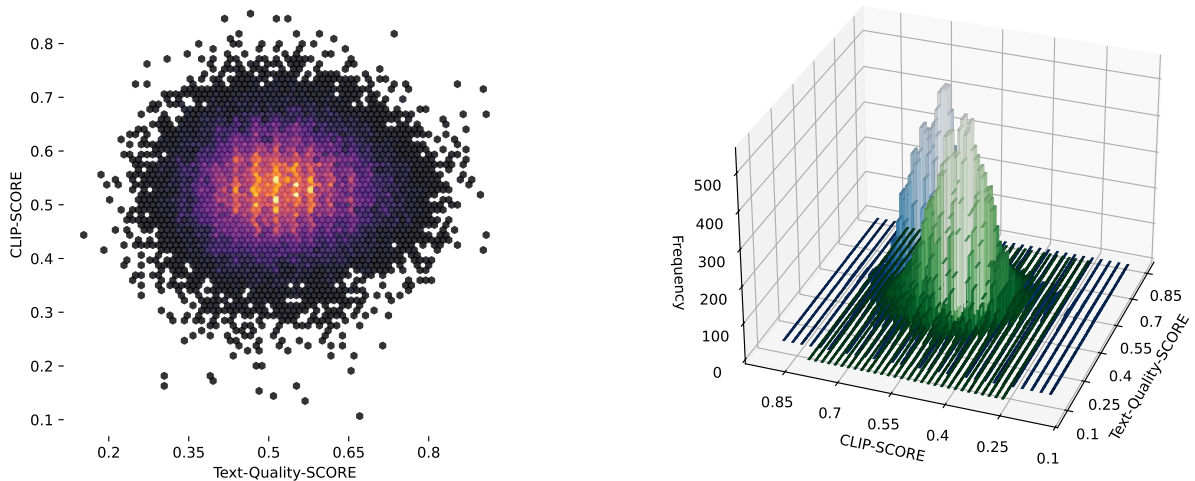


Figure 5: **(Left)** The combined distribution of Text-Quality and CLIP Score. The combined distribution is plotted with Text-Quality Score on the X-axis and CLIP Score on the Y-axis, forming a 2D distribution. The density is illustrated, where lighter colors indicate lower densities and brighter colors represent higher densities. **(Right)** The combined distribution of sampling results of 665K data of LLaVA Stage 2. The same axis settings as the left figure are used, with an additional z-axis representing the data density. The height of the z-axis corresponds to the density of data in the respective region.